

# Thermal conductivity measurement of liquids by means of a microcalorimeter

Benigno Barbés · Ricardo Páramo · Francisco Sobrón · Eduardo Blanco · Carlos Casanova

Received: 29 June 2010/Accepted: 8 November 2010/Published online: 15 December 2010  
© Akadémiai Kiadó, Budapest, Hungary 2010

**Abstract** A study has been carried out of calorimetric cells based on the coaxial cylinder method suitable for the thermal conductivity measurements in a C80D micro-calorimeter from Setaram (France). On the hypothesis of a pure conductive process, it has been possible to obtain the equation expressing the thermal conductivity  $k$  of a liquid sample in function of the heat flow measured by the calorimeter, and the relative thermal conductivity uncertainty has been analysed. To justify the hypothesis of practical absence of convection and negligible temperature differences during experimentation, a CFD (Computational Fluid Dynamics) study has been performed. With a view to testing our equipment and calibration method, the thermal conductivities of some pure liquids (toluene, *n*-decane) and systems (water + ethanol and nanofluid water/Al<sub>2</sub>O<sub>3</sub>), which cover a wide range, have been measured.

**Keywords** Thermal conductivity · Coaxial cylinder method · Micro-calorimeter · Computational fluid dynamics

## Introduction

Thermal conductivity is a property that characterizes the ability of a material to transmit heat and is a macroscopic representation of all the molecular effects that contribute to the conduction of heat through it. In general, thermal conductivity depends on temperature, pressure and nature of the substance. The effects of temperature on the conductivity of solids and liquids are significant and complex.

New technologies developed in the past few decades in electronics, communication, computing, energy production, biomedicine and manufacturing of many types have considerable problems in managing the heat power generated because conventional heat transfer fluids such as air, water, ethylene glycol and light oils have low thermal conductivities. New efficient cooling systems and thermal fluids with greater heat transfer capability are required. With respect to the second option, in the past several years important efforts have been made to enhance the thermal conductivity of heat transfer fluids by dispersing and stably suspending nanometer-sized particles. The study of these thermal fluids, the so-called nanofluids, has emerged as a new field of scientific research with innovative applications. One of the most characteristic properties of a nanofluid is a substantial increase in thermal conductivity and a stronger temperature-dependent thermal conductivity than in the base fluid alone. Extensive experimental research is required into the thermal conductivity of nanofluids before commercial application, and our laboratory has been dedicated to that task during the last year.

Unfortunately, thermal conductivity values are not easy to obtain experimentally. In fact, measurements by different laboratories are often characterized by poor reproducibility and errors of about 2–5% [1–3]. There are two sets of methods for measuring thermal conductivities [4]. In the

B. Barbés · R. Páramo · C. Casanova (✉)  
Departamento de Física Aplicada, Universidad de Valladolid,  
47005 Valladolid, Spain  
e-mail: casanova@termo.uva.es

F. Sobrón  
Departamento de Ingeniería Química, Universidad de  
Valladolid, 47005 Valladolid, Spain

E. Blanco  
Área de Mecánica de Fluidos, Universidad de Oviedo,  
33271 Gijón, Spain

steady-state methods, the temperature remains constant; in the transient methods, the temporal behaviour of the temperature field in the fluid is measured. Amongst all of them, the four that have given the most reliable results are: the parallel plates, the hot wire, the coaxial cylinders and the concentric spheres.

We performed our measurements with the steady-state coaxial cylinders method, using a Setaram C80D microcalorimeter, equipped with calorimetric vessels suitable for thermal conductivities of liquids, also developed by Setaram. This method has the drawback that it is time-consuming; yet, it permits a good temperature control and a very precise measurement of the heat flow which passes through the sample; this is the key measurement that, with a good calibration method, allows accurate and reliable experimental thermal conductivity data to be obtained. This method is also particularly suitable for studying suspensions of nanoparticles in base liquids (nanofluids) because the measurement is made with very small temperature gradients and with practical absence of natural convection, as will be justified later.

The first aim of this article has been to develop a suitable model of the experimental cell to justify the equation which expresses the thermal conductivity of a liquid sample in function of the heat flow measured by the calorimeter. On the basis of that equation the main factors affecting the overall relative thermal conductivity uncertainty have been analysed. As liquids are almost always susceptible to natural convection currents whenever there is a temperature gradient, it is necessary to ensure negligible convection heat transfer and negligible temperature differences during the experiments. The second aim of this article has been to justify that both characteristics are fulfilled in our experimental vessels and to test our experimental procedure.

## Experimental

In order to measure thermal conductivities, a differential heat-flow microcalorimeter C80D from Setaram (France) was used. The basic design of this apparatus is similar to that of a standard Calvet microcalorimeter [5]. The main differences lie in an essentially lighter microcalorimeter block and a lower response time.

The temperature is measured in the calorimetric block, which contains the two vessels, but it does not correspond to the true temperature of the measured sample. The necessary temperature calibration has been undertaken by means of a calibrated 2804A Hewlett-Packard Thermometer, with the quartz probe embedded in a stainless steel block of the same geometry as the vessels. We estimate the final uncertainty of the temperature to be better than  $\pm 0.1$  K.

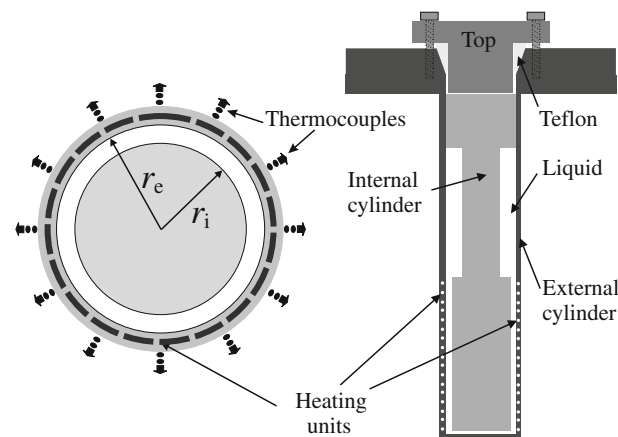


**Fig. 1** Thermal conductivity vessel

To measure thermal conductivities, we used a set of vessels provided by Setaram [6, 7] which fit inside the microcalorimeter. Figure 1 shows an outline of one of them. The internal cylinder—made of copper due to its high thermal conductivity—is in contact with the upper part of the vessel—made of stainless steel—which maintains good thermal contact with the calorimetric block to ensure that the internal cylinder temperature is equal to that of the calorimetric block. A Teflon ring, which is flattened by the pressure of the top, reduces vapour loss at high temperature. The liquid to be measured is poured into the space between the internal and external cylinders.

Inside the lower part of the external cylinder there is a heating wire. By means of a power supply (Agilent E3640A), an electric current passes through the wire, generating a precise defined thermal power by the Joule effect. Part of this power goes through the liquid layer and is evacuated into the internal cylinder. The rest is measured by the thermopile.

Once the calorimeter is at a constant temperature, the experimental procedure consists in leaving the device to attain a steady state for some time (at least 2 h), and determining the heat flow signal corresponding to the base line. Following this, the power supply is turned on, the heat flow signal increases until it reaches a plateau and the heat flow signal is measured again. The difference between the plateau and the base line signals is related to the thermal conductivity of the liquid by an expression we will subsequently deduce.

## Thermal conductivity equation

In this section we deduce the equation which expresses the thermal conductivity  $k$  of a liquid sample inside the cell in function of the heat flow measured by the calorimeter, based on a rigorous model. It is assumed that heat is only

transmitted by conduction. It is obvious that there is no radiation at the temperatures at which we are working (up to 338.15 K). The absence of convection is justified by means of dimensionless constants and following this by a finite volume calculation.

Natural convection in an enclosed space of length  $\delta$  between two cylindrical surfaces exists only [8] if the Rayleigh number  $Ra$ , the product of Prandtl number  $Pr$  and Grashof number  $Gr$  at distance  $\delta$ , is greater than  $10^3$ , with  $Ra_\delta = Gr_\delta \cdot Pr$

$$Gr_\delta = \frac{g\beta}{v^2} \delta^3 \Delta T$$

and

$$Pr = \frac{v}{\alpha}$$

where  $g$  is the gravity acceleration,  $\beta$  is the thermal expansion coefficient,  $v$  is the kinematic viscosity,  $\Delta T$  is the temperature difference between the surfaces and  $\alpha$  is the thermal diffusivity. For water, at temperatures between 298.15 and 363.15 K,  $Ra_\delta$  varies from  $1.9 \times 10^{10}$  to  $7.6 \times 10^{10} \delta^3 \Delta T$ . In our vessel  $\delta = 2.25 \times 10^{-3}$  m and  $\Delta T$  will be less than 0.01 K (calculated for the case of pure convection, with the whole heat flow passing through the liquid, and using the conductivity of water). So  $Ra_\delta < 10$ , and we conclude that there is practically no heat transmission by natural convection.

In Fig. 2, an outline of the measuring cell is shown. The calorimetric block remains at a fixed temperature  $T_b$ . In equilibrium, the cell part with the heating wire reaches a temperature of  $T_c$ , and the lower zone of the inner cylinder a temperature of  $T_{cy}$ . Let us call  $\dot{Q}_s$  the heat flow given by

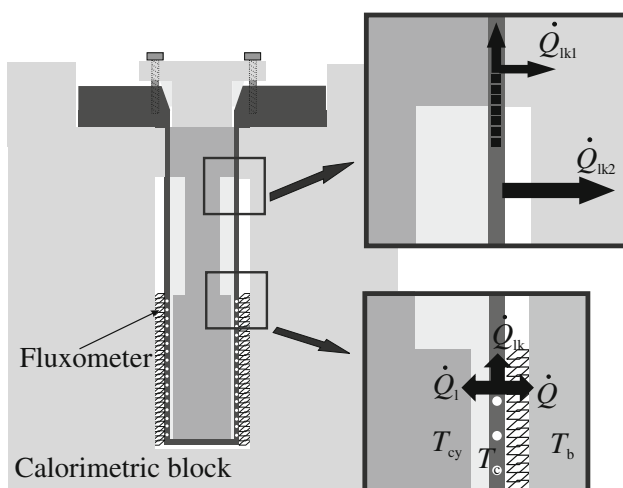


**Fig. 2** Stationary temperatures and heat flows in the thermal conductivity vessel

the power supply;  $\dot{Q}_s$  the heat flow that traverses the liquid layer to the internal cylinder;  $\dot{Q}$  the heat flow conveyed to the thermopile and  $\dot{Q}_{lk}$  the heat flow that reaches the calorimetric block without crossing the thermopile. By energy conservation

$$\dot{Q}_s = \dot{Q} + \dot{Q}_1 + \dot{Q}_{lk} \quad (1)$$

where  $\dot{Q}_s$  is fixed in each experiment and  $\dot{Q}$  is measured. The heat flow between solid surfaces is proportional to the difference of temperatures, so

$$\dot{Q} = C_{tp}(T_c - T_b) \quad (2)$$

The heat flow  $\dot{Q}_1$  that crosses the liquid layer between the concentric cylinders is proportional to the difference in temperatures of the two surfaces,

$$\dot{Q}_1 = kC_l(T_c - T_{cy}) \quad (3)$$

where  $k$  is the thermal conductivity of the liquid and  $C_l$  a constant that depends only on the geometry. Moreover, the heat flow  $\dot{Q}_{lk}$  is evacuated to the calorimetric block through the internal cylinder at the top of the cell, so

$$\dot{Q}_{lk} = C_t(T_c - T_b) \quad (4)$$

As is shown in Fig. 2, a fraction of  $\dot{Q}_{lk}$  (named as  $\dot{Q}_{lk1}$ ) is straightforwardly evacuated to the calorimetric block through the top of the internal cylinder, which maintains a very good thermal contact with the stainless steel cell. On the other hand, the rest (named  $\dot{Q}_{lk2}$ ) flows through the thick liquid layer with a higher thermal resistance, so it is supposed that  $\dot{Q}_{lk2} < < \dot{Q}_{lk1}$ , and then

$$\dot{Q}_{lk} \simeq \dot{Q}_{lk1} = C_{lk}(T_c - T_b) \quad (5)$$

taking into account that  $\dot{Q}_{lk1}$  is a heat flow between two solids in contact.

Resolving the system of Eqs. 1–5, the equation is deduced which expresses the thermal conductivity  $k$  of a liquid sample in function of the heat flow measured by the calorimeter  $\dot{Q}$ :

$$k = \frac{A - \dot{Q}}{B\dot{Q} + C} \quad (6)$$

where the constants  $A$ ,  $B$  and  $C$ , are:

$$A = \dot{Q}_s \frac{C_{tp}}{C_{tp} + C_{lk}} \quad B = \frac{C_l(C_t + C_{tp} + C_{lk})}{C_t(C_{tp} + C_{lk})} \quad C \\ = -\dot{Q}_s \frac{C_l C_{lk}}{C_t(C_{tp} + C_{lk})}$$

These constants depend on the calorimeter temperature, not on the liquid measured. By means of a suitable calibration using three liquids of well-known thermal conductivity: distilled and deionised water [2, 9], glycerol anhydrous (Fluka  $\geq 99.5\%$ ) [1] and *n*-heptane (Fluka,

$\geq 99.5\%$ ) [2, 10], the values of  $A$ ,  $B$  and  $C$  can be obtained as functions of temperature. The three reference liquids have been selected to cover a thermal conductivity range as large as possible.

Equation 6 was proposed by Setaram [7] for their conductivity vessels. Frezzotti et al. [11] obtained the same equation with a more simplified model—no leakage terms—but in which  $A$  corresponds to the constant heat flow provided by the power supply, thus falling in certain incoherence when using  $A$  as a dependent temperature fitting parameter in the calibration process.

### Analyses and evaluation of uncertainties

Let  $\dot{Q}_w$ ,  $\dot{Q}_g$  and  $\dot{Q}_h$  be the values of  $\dot{Q}$  measured for water, glycerol anhydrous and *n*-heptane at a fixed temperature, and  $k_w$ ,  $k_g$  and  $k_h$  their thermal conductivities. For a given temperature, Eq. 6 of the thermal conductivity  $k$  can be expressed as:

$$k = \frac{A - \dot{Q}}{B\dot{Q} + C} = \frac{k_N}{k_D} \quad (7)$$

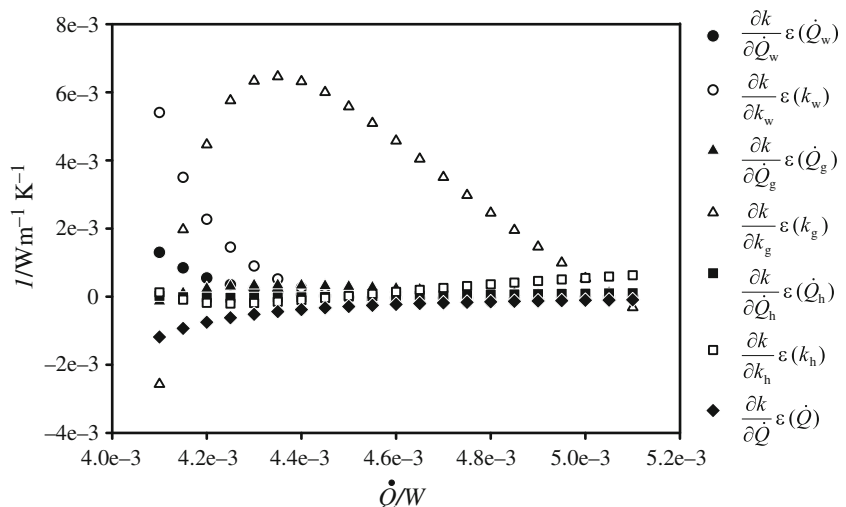
where

$$\begin{aligned} k_N &= \dot{Q}_w \dot{Q}_g k_h (k_w - k_g) + \dot{Q}_w \dot{Q}_h k_g (k_h - k_w) \\ &+ \dot{Q}_g \dot{Q}_h k_w (k_g - k_h) + \dot{Q} \dot{Q}_w k_w (k_g - k_h) \\ &+ \dot{Q} \dot{Q}_g k_g (k_h - k_w) + \dot{Q} \dot{Q}_h k_h (k_w - k_g) \end{aligned} \quad (8)$$

$$\begin{aligned} k_D &= \dot{Q} \dot{Q}_w (k_g - k_h) + \dot{Q} \dot{Q}_g (k_h - k_w) + \dot{Q} \dot{Q}_h (k_w - k_g) + \\ &+ \dot{Q}_w \dot{Q}_g (k_w - k_g) + \dot{Q}_w \dot{Q}_h (k_h - k_w) + \dot{Q}_g \dot{Q}_h (k_g - k_h) \end{aligned} \quad (9)$$

According to Eqs. 7–9  $k = k(\dot{Q}_w, \dot{Q}_g, \dot{Q}_h, k_w, k_g, k_h, \dot{Q})$ , so the uncertainty of  $k$  is assessed by:

**Fig. 3** Partial contributions to the thermal conductivity uncertainty of terms of Eq. 10



$$\begin{aligned} \epsilon(k) &= \sqrt{\sum_{i=w,g,h} \left( \frac{\partial k}{\partial \dot{Q}_i} \right)^2 \epsilon(\dot{Q}_i) + \sum_{i=w,g,h} \left( \frac{\partial k}{\partial k_i} \right)^2 \epsilon(k_i) + \left( \frac{\partial k}{\partial \dot{Q}} \right)^2 \epsilon(\dot{Q})} \end{aligned} \quad (10)$$

where  $\epsilon(\dot{Q}_i)$ ,  $\epsilon(k_i)$  ( $i = w, g, h$ ), and  $\epsilon(\dot{Q})$  are the associated uncertainties of each quantity, and the partial derivatives, which represent the weight of each component in the overall thermal conductivity uncertainty, are given by:

$$\begin{aligned} \left( \frac{\partial k}{\partial \dot{Q}_i} \right) &= k_D^{-2} \left\{ k_D \frac{\partial k_N}{\partial \dot{Q}_i} - k_N \frac{\partial k_D}{\partial \dot{Q}_i} \right\} (i = w, g, h), \\ \left( \frac{\partial k}{\partial \dot{Q}} \right) &= k_D^{-2} \left\{ k_D \frac{\partial k_N}{\partial \dot{Q}} - k_N \frac{\partial k_D}{\partial \dot{Q}} \right\} \end{aligned}$$

and

$$\left( \frac{\partial k}{\partial k_i} \right) = k_D^{-2} \left\{ k_D \frac{\partial k_N}{\partial k_i} - k_N \frac{\partial k_D}{\partial k_i} \right\} (i = w, g, h)$$

According to the literature values used, the relative uncertainties are  $\epsilon_r(k_w) = 0.7\%$  for water [9],  $\epsilon_r(k_h) = 0.5\%$  for *n*-heptane [10] and  $\epsilon_r(k_g) = 2\%$  for glycerol anhydrous [1]. For the temperature interval considered, the reference values used for water and *n*-heptane differ less than 0.5% from those of the correlation equation recommended by IUPAC [2]. In spite of its high uncertainty, glycerol anhydrous has been used in order to cover the normal interval of thermal conductivity values with the three reference liquids. Typical maximum fluctuations of the heat flow signals (base line and plateau) are  $3 \times 10^{-3}$  mW, so we estimate the absolute uncertainty  $\epsilon(\dot{Q})$  as  $6 \times 10^{-3}$  mW for all measurements. For a typical experiment carried out at 308.15 K, Fig. 3 shows the partial contribution to the overall uncertainty, as a function of  $\dot{Q}$ , of the terms in Eq. 10. It is

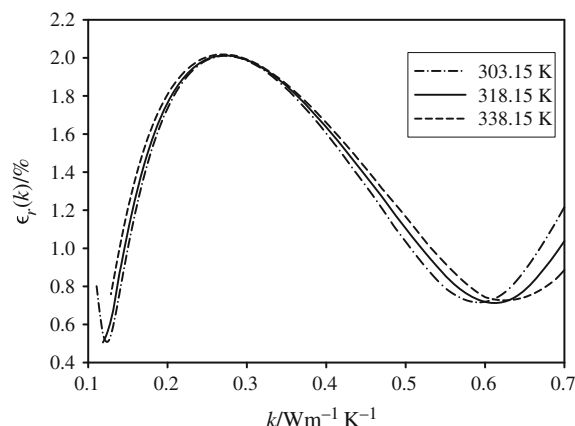


**Fig. 4** Relative thermal conductivity uncertainty in function of the thermal conductivity

worth noting that the principal contribution to uncertainties is due to the literature values of the three reference liquids: more accurate measurements would be possible with more accurate values of reference liquids. Figure 4 represents  $\epsilon_r(k)$  depending on  $k$  at three temperatures. It can be seen that the maximum is near the glycerol anhydrous conductivity value (where  $\epsilon_r(k) \approx \epsilon_r(k_g) = 2\%$ ). In addition, near water the conductivity value  $\epsilon_r(k) \approx \epsilon_r(k_w) = 1\%$ , so this method is very accurate for liquids of conductivities near to water, as is the case of nanofluids with water as the base liquid. Accounting for all the factors, we consider that the overall uncertainty of the present thermal conductivity measurement method is 1.5%.

In order to test our equipment and the calibration method, thermal conductivities of some pure liquids and systems have been measured, which cover a wide thermal conductivity range. Graphical representations of our measurements of the thermal conductivity of toluene (Aldrich,  $\geq 99\%$ ) and *n*-decane (Fluka, purum  $\geq 98\%$ ) in the temperature range from 303.15 to 338.15 K with the corresponding error bar ( $\pm 1.5\%$ ) are given in Figs. 5 and 6, respectively. We have also represented the values (full lines) given by the correlation equations taken from Ramires et al. [12] for toluene and from Assael et al. [10] for *n*-decane. Figure 7 shows our experimental thermal conductivity values of ethanol (Fluka, puriss p.a., absolute  $>99.8\%$ ) and their mixtures with distilled water in function of the composition in weight percentage of ethanol along with very accurate experimental values (uncertainty less than  $\pm 0.5\%$ ) from Assael et al. [13]. Finally, in Fig. 8 thermal conductivity values of the water/ $\text{Al}_2\text{O}_3$  nanofluid at 25 °C with 40–50 nm  $\text{Al}_2\text{O}_3$  nanoparticles (NanoTek®, Alfa Aesar) are presented in function of the nanoparticle volume fraction. We have also represented some of the more recent published data for the same nanofluid in similar conditions. Das et al. [14] used a temperature oscillation technique for the measurement of

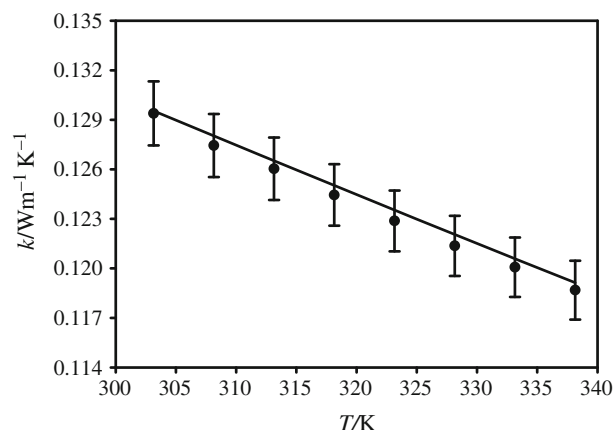


**Fig. 5** Experimental thermal conductivity of toluene. Full curve represents the correlation equation as reported in Ramires et al. [12]

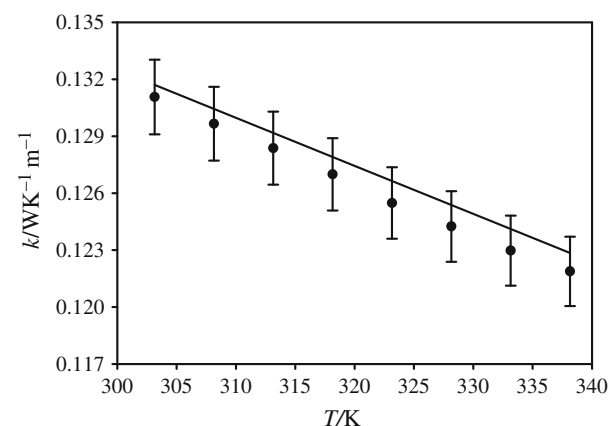


**Fig. 6** Experimental thermal conductivity of *n*-decane. Full curve represents the correlation equation as reported in Assael et al. [10]

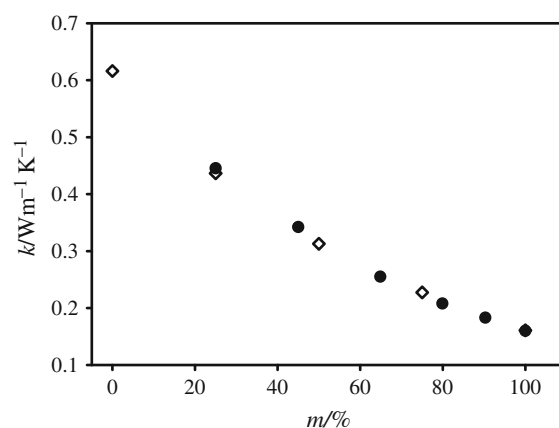


**Fig. 7** Experimental thermal conductivity of ethanol + water mixtures in function of the composition in weight percentage of ethanol: Present work (filled circles), Assael et al. [13] (open diamonds)

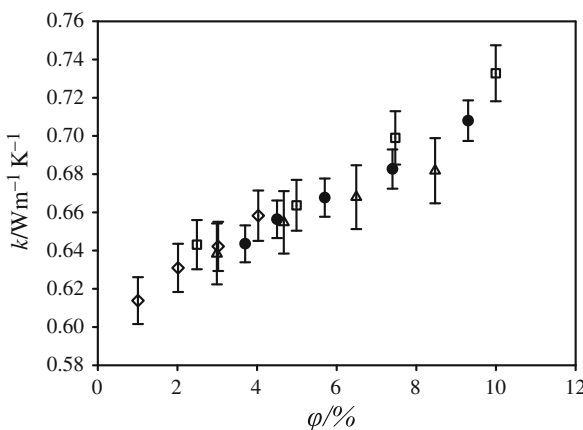


**Fig. 8** Experimental thermal conductivity of the water/Al<sub>2</sub>O<sub>3</sub> nanofluid in function of the nanoparticle volume fraction: Present work at 25 °C (filled circles), Das et al. [14] at 21 °C (open diamonds), Timofeeva et al. [15] at 23 °C (open squares) and Wong et al. [16] at 21 °C (open triangles)

thermal diffusivity, with an uncertainty of  $\pm 2\%$  over the range from 20 to 30 °C, and the thermal conductivity is calculated from it. Their measurements are made at room temperature (21 °C) and the mean nanoparticle diameter is 38.4 nm. Timofeeva et al. [15] made use of a thermal property analyser, model KD2Pro of Decagon Devices, Inc., based on the transient hot wire method, to measure the thermal conductivity of nanofluids at 23 °C with 40–50 nm Al<sub>2</sub>O<sub>3</sub> nanoparticles (NanoDur®, Alfa Aesar). All measurements were performed ten times and averaged, and the error bars drawn in Fig. 8 for this set of data correspond to the standard deviation ( $\pm 2\%$ ) even though the accuracy of the commercial analyser used is  $\pm 5\%$ . Wong et al. [16] used a transient hot wire method to measure the thermal conductivity of 36 nm alumina nanoparticles dispersed in water at 21 °C with an uncertainty of  $\pm 2.5\%$ . It is worth noting that our experimental values are for both pure liquids and systems in very good agreement with the literature values within the reported uncertainties, which give us confidence about our thermal conductivity experimental setup.

## CFD analysis

Since liquids are almost always susceptible to natural convection currents whenever there is a temperature gradient, it is necessary to ensure negligible convection heat transfer and negligible temperature differences during experiments. To justify that both characteristics are fulfilled in our experimental vessels, a CFD (Computational Fluid Dynamics) study has been carried out to obtain the temperature and velocity distribution inside the calorimeter. The FLUENT commercial software has been used. This widely employed CFD code is based on finite

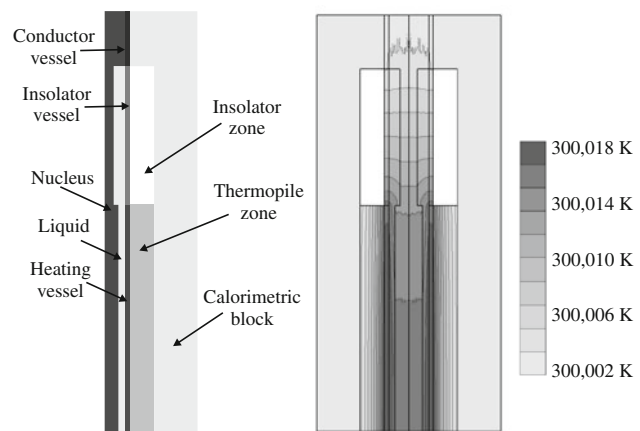


**Fig. 9** **a** Axisymmetric bidimensional model of the thermal conductivity vessel. **b** Temperature distribution inside the calorimeter cell

volumes, and it is capable of resolving the Navier-Stokes equations in the fluid zone and evaluating the heat transfer in adjacent solids.

Taking advantage of the cylindrical symmetry of the vessel, the problem can be reduced to an axisymmetric bidimensional model, shown in Fig. 9a.

From the symmetry axis (Fig. 9a) the following elements are considered:

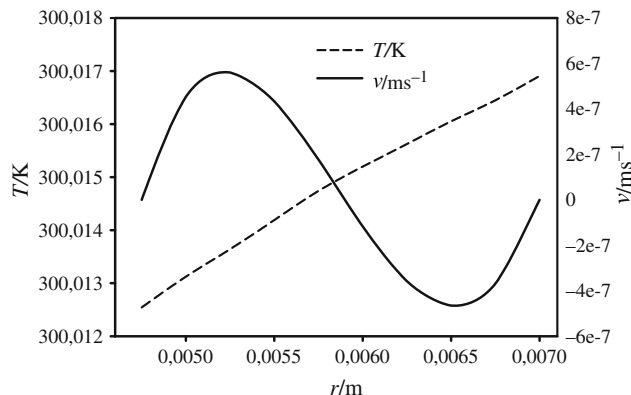
- the cylindrical copper nucleus with three different parts. A wider portion at the top in good contact with the stainless steel vessel, an intermediate part and the part at the bottom;
- the liquid layer;
- the stainless steel vessel, divided into three parts: the lower one containing the heating resistance, separated from the internal copper nucleus through the liquid layer; the middle one, insulated; and the conducting upper part in thermal contact with the nucleus and the calorimetric block;
- the thermopile, between the vessel and the calorimetric block;
- an insulated zone above the thermopile, simulated with adiabatic walls;
- the calorimetric block, made of stainless steel.

The following boundary conditions have been established:

- the external contour of the calorimetric block has a constant temperature;
- the upper and lower limits of the device and the boundaries of the insulated zone are adiabatic;
- the solid interfaces between the copper cylinder and the vessel and between the vessel and the stainless steel wall are supposedly perfect thermal conductors;
- the heating vessel zone is considered a uniform heat source.

**Table 1** Comparison between CFD and analytical calculations for water, glycerol anhydrous and *n*-heptane

Liquid	Model	$(T_c - T_b)/\text{K}$	$(T_{cy} - T_b)/\text{K}$	$\dot{Q}/\text{W}$	$\dot{Q}_l/\text{W}$	$\dot{Q}_{lk}/\text{W}$
Water	CFD	0.0016	0.0123	0.00409	0.00297	0.00073
	Analytical	0.0016	0.0122	0.00411	0.00294	0.00075
Glycerol anhydrous	CFD	0.0174	0.0105	0.00447	0.00252	0.00082
	Analytical	0.0176	0.0108	0.00445	0.00252	0.00082
<i>n</i> -Heptane	CFD	0.0196	0.0077	0.00503	0.00185	0.00092
	Analytical	0.0197	0.0081	0.00504	0.00183	0.00092

**Fig. 10** Temperature and velocity distribution in the middle line of the measured fluid predicted with the CFD model

The mesh is structured with about 68,000 square cells of 0.25 mm side. The flow has been considered of a laminar type. Second-order discretization has been used in all the flow equations. The convergence criteria for the iterative solution required scaled residuals below  $10^{-5}$ .

To test our model we have compared CFD and analytical calculations for water, glycerol anhydrous and *n*-heptane when the calorimetric block temperature  $T_b$  is 300 K, and the heating surface of the vessel releases a calorific power of 7.8 mW. The results are presented in Table 1. There is an excellent agreement between the temperatures at the lower parts of the nucleus ( $T_{cy}$ ) and the vessel ( $T_c$ ) and the flows ( $\dot{Q}$ ,  $\dot{Q}_l$  and  $\dot{Q}_{lk}$ ) predicted by the analytical model and the mean values calculated by the numerical model.

In Fig. 9b, the resulting temperature distribution is shown using water as the fluid. It can be seen that the temperature of the calorimetric block remains constant, except near the thermocouples and in the upper zone in contact with the copper nucleus. As expected, the temperature is almost constant in the lower part of the nucleus and in the heating surface of the vessel. The temperature isolines show that the heat flow is mainly normal to the walls in the zone where the fluid is measured and in the thermopile, as assumed in the analytical model.

The temperature and velocity distribution in the middle line of the measured fluid predicted with the CFD model are plotted in Fig. 10. The temperature profile is nearly linear, as befits a purely conductive heat flow transmission. The velocity profile shape is also the one corresponding to heat conduction, whilst the velocity values are extremely low. Moreover, estimation for the Nusselt number is 0.00027, so the CFD model totally confirms the hypothesis of practical absence of natural convection.

## Conclusions

An extensive study has been made of the calorimetric cells based on the coaxial cylinder method suitable for the thermal conductivity measurements in a C80D microcalorimeter. The main results are:

- An exact equation, based on a rigorous model, has been obtained which expresses the thermal conductivity  $k$  of a liquid sample inside the cell depending on the heat flow measured by the calorimeter.
- According to the calibration method, using three liquids of known thermal conductivity, the factors affecting the overall relative thermal conductivity uncertainty have been analysed.
- Some pure liquids and systems have been measured which cover a wide thermal conductivity range. Toluene and *n*-decane, in the temperature range from 303.15 to 338.15 K. Mixture (water + ethanol) at 303.15 K and the water/ $\text{Al}_2\text{O}_3$  nanofluid at 25 °C with 40–50 nm  $\text{Al}_2\text{O}_3$  nanoparticles. All the experimental values are in very good agreement with the literature values within the reported uncertainties.
- A CFD (Computational Fluid Dynamics) study has been carried out to obtain the temperature and velocity distribution inside the calorimetric cell. The temperature profile calculated corresponds to a purely conductive heat flow transmission and the velocity values are extremely low. This confirms the hypothesis of practical absence of natural convection during the thermal conductivity measurements.

**Acknowledgements** The authors acknowledge Ministerio de Educación y Ciencia (Grant No. CTQ2006-15537-C02/PPQ), Spain, for financial support.

## References

1. Vargaftik AB, Filippov LP, Tarzmanov AA, Totskii EE. Handbook of thermal conductivity of liquids and gases. Boca Raton: CRC Press Inc; 1994.
2. Le Neindre B. Thermal conductivity. In: Marsh KN, editor. Recommended reference materials for the realization of physicochemical properties. Oxford: Blackwell Scientific Publications; 1987. p. 321–70.
3. Labudová G, Vozárová V. Uncertainty of the thermal conductivity measurement using the transient hot wire method. *J Therm Anal Cal.* 2002;67:257–65.
4. Tian F, Sun L, Venart JES, Prasad RC, Mojumdar SC. Development of a thermal conductivity cell with nanolayer coating for thermal conductivity measurement of fluids. *J Therm Anal Cal.* 2008;94(1):37–43.
5. Calvet E, Prat H. Microcalorimétrie. Applications Physico-Chimiques et Biologiques. Paris: Masson et Cie; 1956.
6. Le Parlouër P, Rouyer M, Python F. New experimental vessels for calorimetric investigations of gases and liquids on the Setaram C 80. *Thermochim Acta.* 1985;92:375–8.
7. Python F, Rouyer M. Vapour pressure, heat of evaporation and thermal conductivity determination by means of the C 80 microcalorimeter. *Thermochim Acta.* 1987;14:91–6.
8. MacGregor RK, Emery AF. Free convection through vertical plane layers—moderate and high Prandtl number fluids. *J Heat Transfer.* 1969;91(3):391–403.
9. Ramires MLV, Nieto de Castro CA, Nagasaka Y, Nagashima A, Assael MJ, Wakeham WA. Standard reference data for the thermal conductivity of water. *J Phys Chem Ref Data.* 1995;24(3):1377–81.
10. Assael MJ, Charitidou E, Nieto de Castro CA, Wakeham WA. The thermal conductivity of *n*-hexane, *n*-heptane and *n*-decane by the transient hot-wire method. *Int J Thermophys.* 1987;8(6):663–70.
11. Frezzotti D, Goffredi G, Bencini E. Thermal conductivity measurements of cis- and trans-decahydronaphthalene isomers using a steady-state coaxial cylinders method. *Thermochim Acta.* 1995;265:119–28.
12. Ramires MLR, Nieto de Castro CA, Perkins RA, Nagasaka Y, Nagashima A, Assael MJ, Wakeham WA. Reference data for the thermal conductivity of saturated liquid toluene over a wide range of temperature. *J Phys Chem Ref Data.* 2000;29(2):133–9.
13. Assael MJ, Charitidou E, Wakeham WA. Absolute measurements of the thermal conductivity of mixtures of alcohols with water. *Int J Thermophys.* 1989;10(4):793–803.
14. Das SK, Putra N, Thiesen P, Roetzel W. Temperature dependence of thermal conductivity enhancement for nanofluids. *J Heat Transfer.* 2003;125:567–74.
15. Timofeeva EV, Gavrilov AN, McCloskey JM, Tolmachev YV. Thermal conductivity and particle agglomeration in alumina nanofluids: experiment and theory. *Phys Rev E.* 2007;76:061203.
16. Wong K-FV, Kurma T. Transport properties of alumina nanofluids. *Nanotechnology.* 2008;19:345702.